



IUTAM Symposium on Storm Surge Modelling and Forecasting

Impact of the interaction of surge, wave and tide on a storm surge on the north coast of Vietnam

Tran Hong Thai^a, Nguyen Ba Thuy^{b*}, Vu Hai Dang^c, Sooyoul Kim^d, Lars Robert Hole^e

^aNational Hydrometeorological Service of Vietnam, No8 Phao Dai Lang, Dong Da, Hanoi, Vietnam

^bVietnam National Hydrometeorological Forecasting Center, No8 Phao Dai Lang, Dong Da, Hanoi, Vietnam

^cInstitute of Marine Geophysics and Geology, No18 Hoang Quoc Viet, Cau Giay, Hanoi, Vietnam

^dGraduate School of Engineering, Tottori University, Koyama-cho Minami, Tottori, 680- 850, Japan

^eDivision of Oceanography and Maritime Meteorology, Norwegian Meteorological Institute, Bergen, Norway

Abstract

In the present paper, the interaction of surge, wave and tide on the north coast of Vietnam is assessed using a coupled model of surge, wave and tide. A series of storm surge simulations for Typhoons Frankie (1996) and Washi (2005) are carried out, considering the effects of the tide and the wave that combines a wave dependent drag and wave-induced radiation stress to find out a predominant factor in the storm surge generation. Typhoon Frankie is landfalled at the low tide while Typhoon Washi landfalled at the high tide. The results indicate that the effect of the wave is crucial to the storm surge simulation. In particular, the wave induced-surge improves the accuracy of the storm surge level up to 30 %. It also shows that the surge induced by wave radiation stress is dependant with the space resolution, and the finest resolution is improved and in close agreement with the observation. On the other hand, the influence of the tide is ignorable for the case of Typhoon Frankie and considerable in the case of Typhoon Washi.

© 2017 The Authors. Published by Elsevier B.V.

Selection and peer-review under responsibility of IUTAM Symposium on Storm Surge Modelling and Forecasting.

Keywords: Typhoon; storm surge; a coupled model of surge; wave and tide; interaction of surge

* Corresponding author. Tel.: 84-4-38241600; fax: 87-438241600.

E-mail address: thuybanguyen@gmail.com

1. Introduction

To assess storm surges, there are two conventional types of physics-based numerical models: a decoupled model of storm surge, and a coupled model of surge, wave and tide. In the last three decades, coupled models have been paid attention to, especially focusing on the interaction of surge, wave and tide. Several studies have introduced wind stress as a function of waves (*e.g.*, Janssen^{1,2}). Since then, a number of studies that examined wave-induced stress that is directly obtained in coupled models of surge and wave showed the significant improvements of the model results while comparing with observation data (*e.g.*, Funakoshi, Hagen, and Bacopoulos³; Kim, Yasuda, and Mase⁴; Zhang and Li⁵). Wave setup driven by a force of the divergence of radiation stress in the nearshore has also been studied with coupled models of surge and wave (*e.g.*, Bertin *et al.*⁶; Kim, Yasuda, and Mase⁷; Mastenbroek, Burgers, and Janssen⁸). It was found that the wave setup induced by the force of the radiation stress is substantial in the peak surge level during Typhoon Anita 1970 (*e.g.*, Kim, Yasuda, and Mase⁷). It was investigated that the tide-surge interaction is not negligible when estimating local surge levels (*e.g.*, Chen, Wang, and Zhao⁹; Choi, Eum, and Woo¹⁰; Kim, Yasuda, and Mase⁴). Besides the interaction of tide, wave and surge, topographic characteristics (*e.g.*, bed slope) also plays an important role in the increase or decrease of wave setup, runup and wind driven surge (*e.g.*, Dietrich *et al.*¹¹; Kennedy *et al.*¹²).

For several decades, climate change impact studies have focused on storm surge studies in Vietnam (*e.g.*, Ninh¹³; Sao¹⁴; Thuy¹⁵). Conventional ways of two (or three) dimensional nonlinear shallow water equations have been used. In other words, in those studies other factors such as tides and waves were not taken into account in the storm surge model. Recently, the effect of waves on storm surge has been investigated in Vietnam. Hien *et al.*¹⁶ showed that the wave setup induced by the force of the divergence of radiation stress is significant in the storm surge on the coast of Haiphong using empirical formula. Thuy *et al.*¹⁷ found that the Typhoon Kalmaegi (2014) surge was significantly influenced by the waves on the Haiphong coast in Vietnam, obtained from numerical simulations using a coupled model of surge, wave and tide.

In the present study, the primary factors affecting storm surge on the north coast of Vietnam are quantitatively investigated using a coupled model of surge, wave and tide. In the study area, the tidal cycles are *diurnal* and the maximum tidal range is up to 3.6 m. Therefore, the tide is also taken into account in the simulation. The study highlights that coupling processes between surge and wave are critical to the prediction of storm surge on the north coast of Vietnam and only using a coupled model of surge, wave and tide (*e.g.*, SuWAT developed by Kim *et al.*⁴) is able to accurately estimate storm surges. A series of storm surge simulations are conducted for Frankie (1996) and Washi (2005) that consider the interaction of surge, wave and tide.

2. Method

To analyze the storm surge in the study area, the coupled model of surge, wave and tide (called SuWAT), developed by Kim, Yasuda, and Mase⁴ was used. SuWAT is capable of doing parallel computations for an arbitrary number of domains using the Message Passing Interface (MPI). In the present study, three modules of surge, wave and tide are integrated into SuWAT as shown in Figure 1 that reveals the information of the flow among the modules and the domains. The tidal module provides only boundary conditions to the surge modules in the outermost domain. Coupling parameters include open boundary values, internal exchange among modules and domains in a machine. The calculations are sequentially carried out from the higher level domain to the lower level; the rest of the lower level domains wait for the completion of the higher level domain at a time step. This modeling system has been implemented and verified in other studies (*e.g.*, Kim, Yasuda, and Mase⁷; Kim *et al.*^{18,19}; Mase *et al.*²⁰).

2.1. Surge module

The surge module solves the depth averaged nonlinear shallow water equations using the staggered Arakawa C grid in space and the leap frog scheme in time. The explicit finite difference scheme is used with the upwind method:

$$\frac{\partial \eta}{\partial t} + \frac{\partial M}{\partial x} + \frac{\partial N}{\partial y} \quad (1)$$

$$\frac{\partial M}{\partial t} + \frac{\partial}{\partial x} \left(\frac{M^2}{d} \right) + \frac{\partial}{\partial y} \left(\frac{MN}{d} \right) + gd \frac{\partial \eta}{\partial x} = fN - \frac{1}{\rho_w} d \frac{\partial P}{\partial x} + \frac{1}{\rho_w} (\tau_s^x - \tau_b^x - F_x) + A_h \left(\frac{\partial^2 M}{\partial x^2} + \frac{\partial^2 M}{\partial y^2} \right) \quad (2)$$

$$\frac{\partial N}{\partial t} + \frac{\partial}{\partial y} \left(\frac{N^2}{d} \right) + \frac{\partial}{\partial x} \left(\frac{NM}{d} \right) + gd \frac{\partial \eta}{\partial y} = -fM - \frac{1}{\rho_w} d \frac{\partial P}{\partial y} + \frac{1}{\rho_w} (\tau_s^y - \tau_b^y - F_y) + A_h \left(\frac{\partial^2 N}{\partial x^2} + \frac{\partial^2 N}{\partial y^2} \right) \quad (3)$$

where η is the sea surface level, M and N are the components of depth-integrated velocity in the horizontal and vertical directions, P is the atmospheric pressure, f is the Coriolis parameter, g is the gravitational acceleration, d is the total water depth ($\eta + h$), A_h is the horizontal eddy diffusions, ρ_w is the density of water, and F_x and F_y represent the components of wave force which correspond to the gradients of wave-induced radiation stress:

$$F_x = \frac{-\partial S_{xx}}{\partial x} - \frac{\partial S_{xy}}{\partial y} \quad (4)$$

$$F_y = \frac{-\partial S_{yx}}{\partial x} - \frac{\partial S_{yy}}{\partial y} \quad (5)$$

where the wave radiation stresses are expressed by:

$$S_{xx} = \rho g \iint \left[\frac{C_g}{c} \cos^2 \theta + \frac{C_g}{c} - \frac{1}{2} \right] E d\sigma d\theta \quad (6)$$

$$S_{xy} = S_{yx} = \rho g \iint [\cos \theta \sin \theta] E d\sigma d\theta \quad (7)$$

$$S_{yy} = \rho g \iint \left[\frac{C_g}{c} \sin^2 \theta + \frac{C_g}{c} - \frac{1}{2} \right] E d\sigma d\theta \quad (8)$$

where C and C_g are the wave velocity and the group velocity, σ and θ are the angular frequency and the wave direction, and E is the energy, density, and spectrum respectively. A conventional quadratic law is applied to the sea surface and bottom boundary layers. The bottom stress is computed by:

$$\tau_b = \rho_w g n^2 \frac{\vec{Q}|\vec{Q}|}{d^{7/3}} \quad (9)$$

In which \vec{Q} is the depth-integrated velocity vector, and n is the Manning number (0.025) in all the domains, as determined by Chien²¹. The wind stress is usually estimated by the following equation:

$$\tau_s = \rho_a C_D \vec{U}_{10} |\vec{U}_{10}| \quad (10)$$

where ρ_a is the density of air, C_D is the drag coefficient and \vec{U}_{10} is the wind speed at 10 m height. In a series of storm surge simulations, two C_D s are used. One is the conventional C_D (Honda and Mitsuyasu²²):

$$C_D = \begin{cases} (1.290 - 0.024W) \times 10^{-3} & (W \leq 8 \text{ m/s}) \\ (0.58 + 0.063W) \times 10^{-3} & (W > 8 \text{ m/s}) \end{cases} \quad (11)$$

The other is the wave dependent C_D (Janssen^{1,2}). In SuWAT, Mastenbroek, Burgers, and Janssen's⁸ iteration for Janssen's formulation of the exponential wave growth term in wave modules, (given in the section of Wave module), is used to estimate the wave dependent C_D . Following his assumption, waves influence the boundary layer: $\tau = \tau_w + \tau_\tau$, where τ_w is the wave-induced stress, τ_τ the turbulent stress and τ the total stress. The wind profile is given by:

$$U(z) = \frac{u_*}{\kappa} \ln \left(\frac{z+z_e+z_0}{z_e} \right) \quad (12)$$

where $U(z)$ is the wind speed at height, z_e is the effective roughness, z_0 is the roughness length, z is the height and $\kappa=0.4$ is the von Kármán constant. The turbulent stress is parameterized with a mixing-length hypothesis:

$$\tau_t = \rho_a (\kappa z)^2 \left(\frac{\partial U}{\partial z} \right)^2 \quad (13)$$

where ρ_a is the air density. If the wind profile (12) is differentiated, squared and compared with the form (13), an expression for z_e for $z = z_0$ (Mastenbroek, Burgers, and Janssen⁸) can be found:

$$z_e = \frac{z_0}{\sqrt{1-\tau_w-\tau}} \quad (14)$$

where: $\tau_w = \tau_w(z_0)$. To parameterize the roughness length z_0 , Janssen assumes that a Charnock-like relation $z_0 = \tilde{\alpha} u_*^2/g$ is valid with the values for $u_* = \sqrt{\tau/\rho_a}$ and $\tilde{\alpha} (=0.0081)$, the Charnock parameter. With the effective roughness (z_e), the wave dependent C_D is finally obtained by Eq. (15):

$$C_D = u_*^2 / U(z)^2 = \left[\kappa / \ln \left(\frac{z+z_e-z_0}{z_e} \right) \right]^2 \quad (15)$$

In this study, Eq. (15) is used to estimate the wind stress in Eq. (10) instead of the conventional C_D in Equation (11). The effect of levelling off at wind speeds of 22-33 m/s on C_D is not taken into account (Donelan *et al.*²³; Kim *et al.*¹⁹).

The solid boundary condition is adopted at land boundaries for no inundation conditions. The radiation condition along open boundaries is given by following Flather's method²⁴ in all the domains. The current and sea surface level in the coarse grid domain are transferred to the nested open boundaries in the fine grid domain at each time step of 4 s. The time step is 4 s for the surge model.

2.2. Tidal module

The astronomical tide in SuWAT is imposed by a global ocean tide model (Matsumoto, Takanezawa, and Ooe²⁵) that predicts tidal levels for sixteen constituents of M2, S2, K1, O1, N2, P1, K2, Q1, M1, J1, OO1, 2N2, Mu2, Nu2, L2 and T2. At every time step, the tidal level is imposed on open boundaries in only the outermost domain. Along the open boundary, the sea surface level is given by:

$$\eta = \eta_{tide} + \eta_{surge} \quad (16)$$

where η_{tide} is the tidal level and η_{surge} is the surge level.

2.3. Wave module

The wave model of Simulating WAVesNearshore (SWAN; Booij, Ris, and Holthuijsen²⁶) integrated in the wave module solves the spectral action balance equation to estimate a wave spectrum (Booij, Ris, and Holthuijsen²⁶). The wave in SuWAT is estimated by time varying currents and sea surface levels calculated from the surge module. The updated parameters of the wave dependent drag and the radiation stress in the wave module are returned to the surge module to calculate the current and sea surface level. The SWAN version 40.41 has been integrated into SuWAT as the wave module (Kim, Yasuda, and Mase⁴).

As done in Kim *et al.*¹⁹, in the present simulation, the default values of parameters for the physics are used: Cavaleri and Malanotte-Rizzoli²⁷ for linear wave growth, Janssen^{1,2} for exponential wave growth, Janssen² for white-capping, Hasselmann *et al.*²⁸ for quadruplet interaction, Battjes and Janssen²⁹ for depth-induced breaking and

Madsen, Poon, and Graber³⁰ for bottom friction. The diffraction is adapted in the wave calculation. An Ursell number of 10 is used for the limit of the quadruplet interaction with a factor of 1.0 for the fraction of breaking waves. The following discretizations were used: the direction resolution is 10° and the frequency range is 0.05 to 1.00 Hz. In the outermost domain, the wave spectrum along open boundaries is estimated by the JONSWAP spectrum with the peak enhancement parameter of 3.3, the peak period and the directional width of 10°. The wave spectrum in the coarse grid domain is transferred to the open boundaries in the fine grid domain at each time step of 900 s. The time step is 900 s for the wave model.

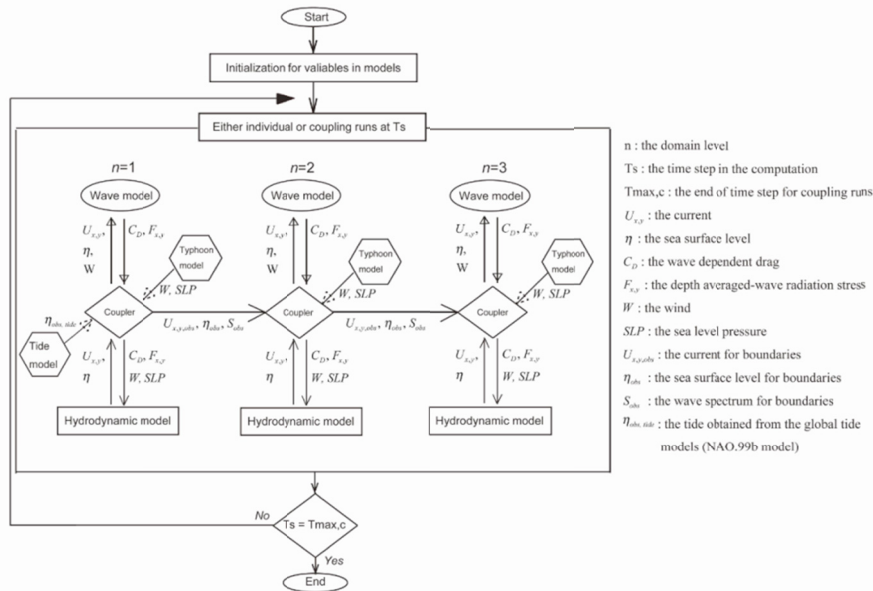


Fig. 1. Framework of SuWAT for three level domains that shows the information flow between surge and wave modules in each domain.

2.4. Parametric wind and pressure model

A parametric wind and pressure model implemented in the SuWAT model is used to estimate typhoon wind and pressure fields. Schloemer’s formula³¹ is used for the pressure:

$$p = p_c + \Delta p \exp(-r_0/r) \tag{17}$$

where p is the atmospheric pressure at a distance r from the center, p_c is the central atmospheric pressure, Δp is the difference between p and p_c , and r_0 is the radius to the maximum wind.

Fujii and Mitsuta’s formula³² for the surface wind is written as follows:

$$V_{gr} = r_t \left(\sqrt{\frac{f^2}{4} + \frac{r_0 \Delta p}{\rho_a r^2 r_t} \exp(-r_0/r)} - \frac{f}{2} \right) \tag{18}$$

where V_{gr} is the geostrophic wind and r_t is the following relation,

$$r_t = r / \left(1 + \frac{U_{10}}{V_{gr}} \sin \beta \right) \tag{19}$$

In Eq. (19) V_{gr} and U_{10} are at the previous time step. β is the degree between the typhoon moving direction and the direction to r in the anti-clockwise direction. U_{10} is calculated by multiplying V_{gr} by $G(x)$ as follows:

$$G(x) = G(\infty) + [G(x_p) - G(\infty)](x/x_p)^{k-1} \exp\left\{(1 - 1/k) \left[1 - (x/x_p)^k\right]\right\} \quad (20)$$

$$U_{10} = V_{gr} G(x) \quad (21)$$

where: $x = r/r_0$, $k = 2.5$, $x_p = 0.5$, $G(x_p) = 1.2$ and $G(\infty) = 0.667$ are given by Fujii and Mitsuta³². In the wind model, the geostrophic wind is reduced by a factor of $G(\infty)$. Finally, the wind at 10 m height is obtained from the vector sum of the wind at 10 m height calculated by Eq. (21) and the typhoon moving speed. In the present model, deformation of the core structure in the typhoon is not considered.

2.5. Bathymetry

For numerical simulations, the complexity of the geophysical features was taken into account using the three level grid system, where the outermost domain, D1, (Fig. 2 (a)) covers the whole East Sea and the domain, D2, (Fig. 2 (b)) is set to cover the northern coast of Vietnam. The innermost domain, D3 (Fig. 2 (c)), is focused on stations of Hondau. General Bathymetry Chart of the Ocean (GEBCO) of British Ocean Data Center was used to extract bathymetry for the domains of D1 and D2. On the other hand, coastal topography maps with scales of 1/100,000 published from the Vietnam Administration of Seas and Islands were used for the domain D3. The space resolutions for D1, D2 and D3 in both X and Y direction is 7400m, 1850m, and 825m.

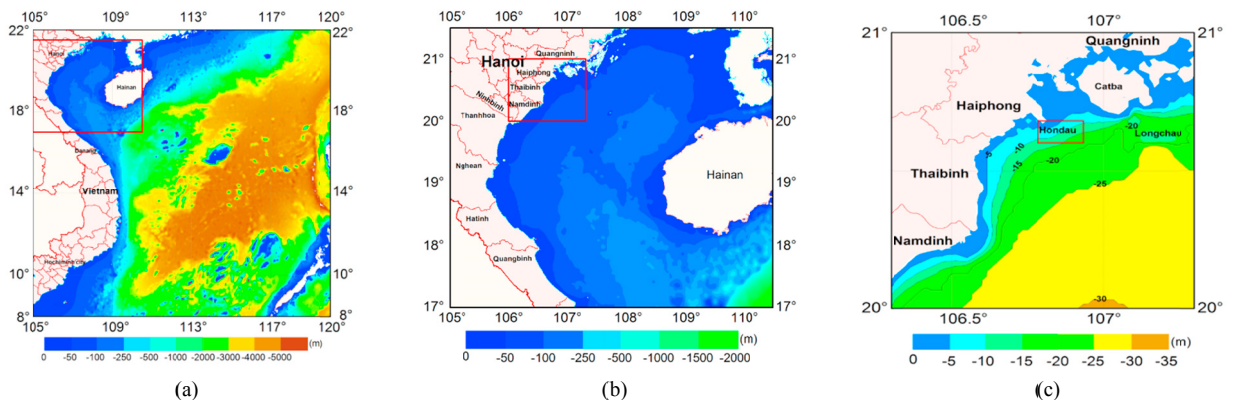


Fig. 2. Geophysical domains of the study area with three levels. (a) shows the outermost domain of the Vietnam coast. (b) shows the intermediate domain. (c) focuses on the innermost domain with Hondau station.

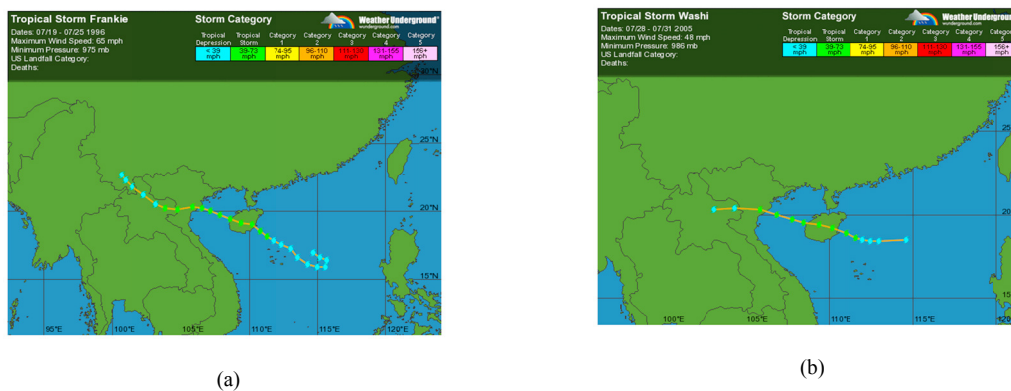


Fig. 3. Track of Typhoon (a) Frankie (1996), (b) Washi (2005).

3. Results

To examine a critical factor to the generation of storm surge in the north coast of Vietnam, the representative historical typhoons of Frankie (1996) and Washi (2005) were selected. These typhoon tracks are provided in Fig. 3. Typhoon Frankie landfalled at the low tide while Typhoon Washi landfalled at high tide as the time profile of total water level observation, tide predict and storm surge at Hondau station in both typhoon cases showed in Fig. 4.

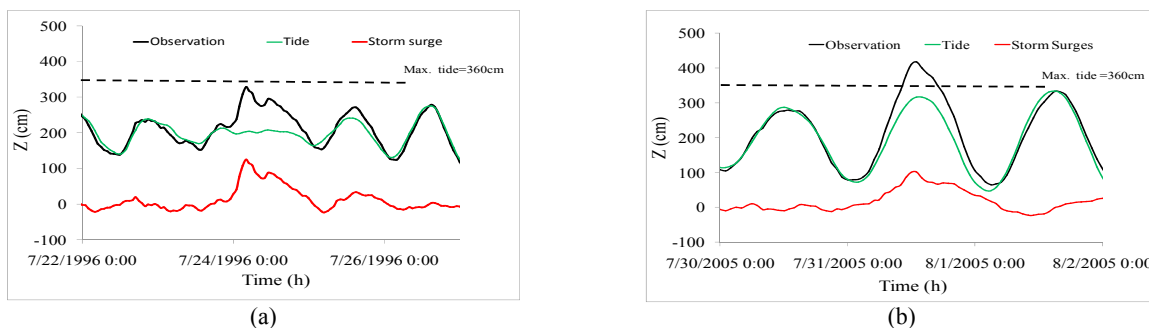


Fig.4. Time serial of total water level (observation), predicted tide and storm surge at Hondau station during Typhoon Frankie (a) and Washi (b).

3.1. Impact of the tide on the storm surge

In order to investigate how the tide influences the storm surge in the study area, a series of simulations were conducted using SuWAT that the surge and tide interaction was taken into account to calculate the Typhoon Frankie and Washi surge. In the storm surge simulation, the conventional C_D (Honda and Mitsuyasu²²) was used to estimate the wind stress. First, the surge simulation was carried out with the tide. Then, only the tide simulation was conducted to extract the surge level taking into account the surge and tide interaction. Finally, only the surge simulation without the tide was executed on mean sea level. With two surge levels, the effect of the tide on the storm surge is examined as shown in Fig. 5(a) and (b) that show a comparison of observations and calculations at Hondau. From the results of simulation, the effect of tide on storm surge in the case of Typhoon Frankie is very small, with a difference of about 3%. In the case of Typhoon Washi, the case considering the tide effect giving the pick surge is lower than the case without considering the tide effect with a difference of about 13%. This is due to Typhoon Washi landfalled at the high tide that the water deep is higher in the mean sea level. In addition, it indicates that the use of the conventional C_D in both cases is not enough to simulate the observations, regardless of the consideration of the surge and tide interaction. As a result, it was found that the tidal effect is significant in the surge level on the coast of study area when typhoon lanfalled is at the high tide.

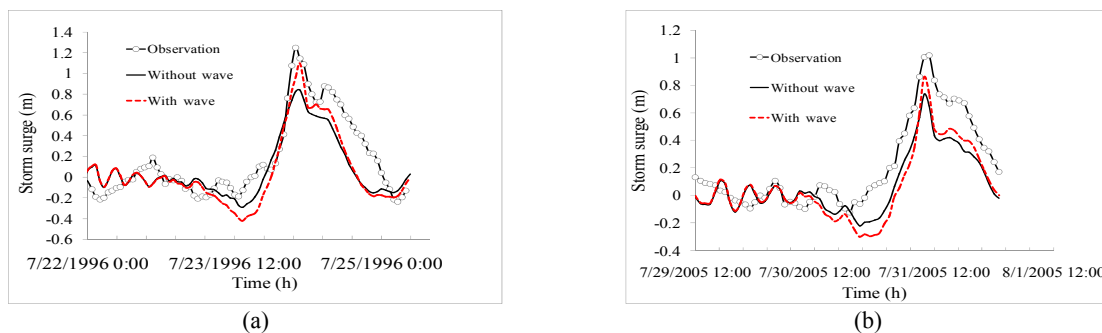


Fig.5. Comparisons of the observations and calculations with and without the tide in the surge simulations of Typhoon Frankie (a) and Whashi at Hondau station.

3.2. Impact of the wave on the storm surge

The effect of wave on storm surge was discussed for the case of the storm surge simulation running coupled and uncoupled surge and wave. This case was calculated using both of the wave dependent drag and the radiation stress on mean sea level, and then compared with that obtained from the run using only the conventional drag on mean sea level, as shown in Fig. 6 (a) and (b). From the results, it is seen that the peak surge level calculated with the wave effect is in close agreement with the observation at Hondau in both cases. The difference between them is about 0.3 m in both typhoon cases. Thus, it can be said that the surge and wave interaction apparently improves the surge level.

Figures 7(a) and (b) show the spatial distribution of the peak surge levels in the case of uncoupled surge with wave (a) and coupled surge with wave (b). It could be found that, in the case of the coupled surge with wave, the maximum surge level is higher and the area of storm surge is extended, in comparison with the case uncoupled with wave.

The effect of wave induced radiation stress (wave setup) is however depended on the space resolution. Although the space resolution used in the above figures is fine (925m) for conventional storm surge simulation, the result of peak surge is still underestimated in both typhoon cases. It may be due to the underestimation of wave setup estimated on the coarse resolutions. To concrete our finding, the additional simulations of the Typhoons Frankie surges were conducted for five cases of space resolution (450m (D4), 150m (D5)). It can be seen that, the peak surge is increased as the space resolution is increased, and is in close agreement with the observation data (Fig. 8). Hence, further studies should be done on higher resolutions of less than 1 km grid size when planning and managing coastal facilities and structures.

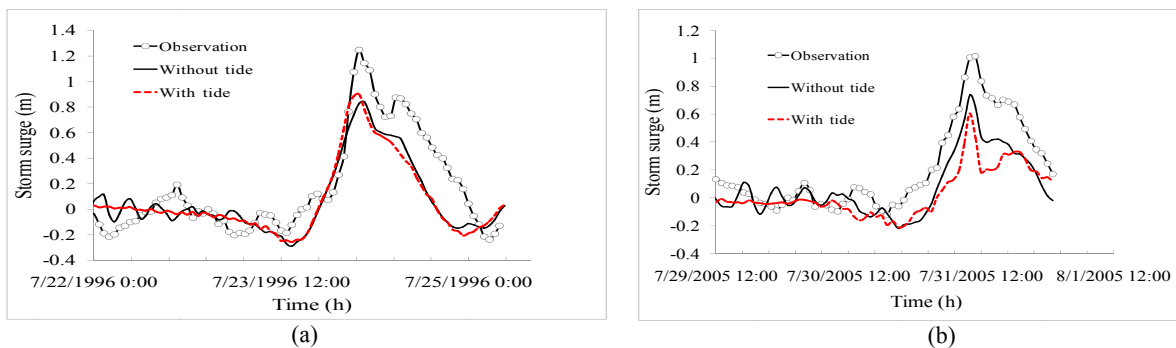


Fig. 6. Comparisons of the observations and calculations with and without the wave effect in the surge simulations of Typhoon Frankie (a) and Whashi (2005) at Hondau station.

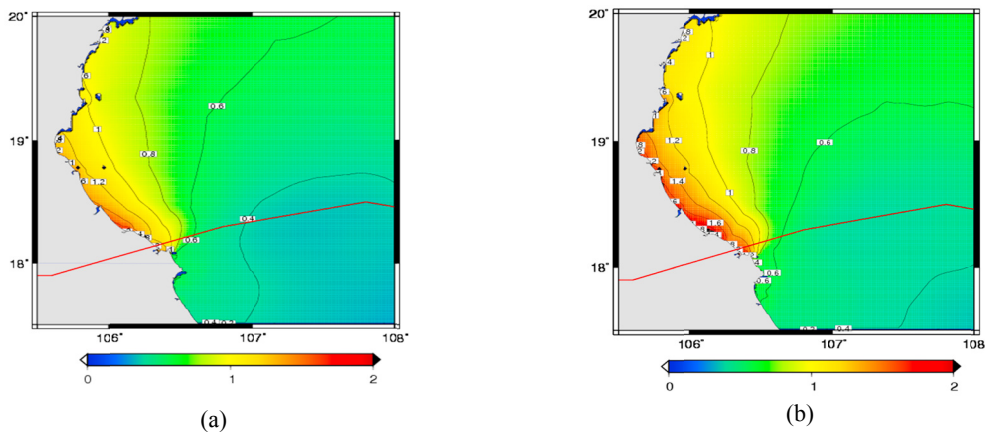


Fig.7. Spatial distributions of the peak surge levels due to Typhoon Washi for the case uncoupled (a) and coupled with wave(result in domain D2).

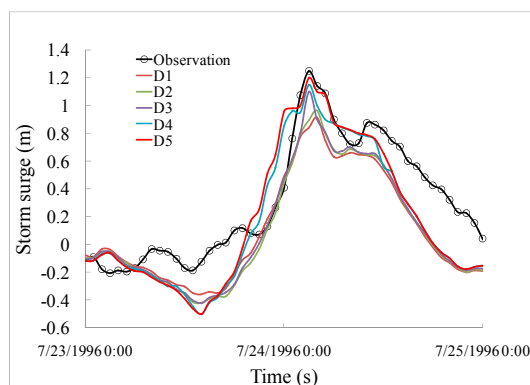


Fig. 8. Time serial of storm surge at Hondau station due to Typhoon Washi (2005) in six cases of space resolution.

4. Conclusions

The interaction of surge and tide is investigated during Typhoon Frankie (1996) and Washi (2005) landfalled at the north coast of Vietnam, where the maximum tidal range is up to 1.8 m. It indicates that the effect of the tide on the surge is ignorable for the case of Typhoon Frankie landfalled at low tide, and it is significant in the case of Typhoon Washi landfalled at the high tide with a difference of 13 % between the surge levels with and without the tide. For the surge and wave interaction, two factors of the wave dependent drag and the wave-induced radiation stress are focused in the surge simulation. It is shown that, the wave and surge interaction combining the wave dependent drag and the radiation stress contributes 30% of the total surge level and is crucial to simulating the storm surge. It also shows that, the surge induced by wave radiation stress is dependent on the space resolution, and the finest resolution is improved and in close agreement with the observation. Hence, further studies should be done on higher resolutions of less than 1 km grid size when planning and managing coastal facilities and structures.

Acknowledgements

This research is funded by Vietnam National Foundation for Science and Technology Development (NAFOSTED) under grant number 105.06-2017.07, partially supported by JSPS KAKENHI Grant Number 15549699 and the Norwegian Ministry for Foreign Affairs (Hole).

References

- Janssen PAEM. Wave-induced stress and the drag of air flow over sea waves. *Journal of Physical Oceanography* 1989;**19**:745-754.
- Janssen PAEM. Quasi-linear theory of wind-wave generation applied to wave forecasting. *Journal of Physical Oceanography* 1991;**21**: 1631-1642.
- Funakoshi Y, Hagen SC and Bacopoulos P. Coupling of hydrodynamic and wave models: case study for Hurricane Floyd (1999) hindcast. *Journal of Waterway, Port, Coastal, and Ocean Engineering* 2008;**134**(6):321-335.
- Kim SY, Yasuda T, and Mase H. Numerical analysis of effects of tidal variations on storm surges and waves. *Applied Ocean Research* 2008; **30**:311-322.
- Zhang MY and Li YS. The dynamic coupling of a 3rd-generation wave model and a 3D hydrodynamic model through boundary-layers. *Continental Shelf Research* 1997; **17**:1141-1170.
- Bertin X, Li K, Roland A and Bidlot JR. The contribution of short waves in storm surges: two recent examples in the central part of the bay of Biscay. *Continental Shelf Research* 2015;**96**:1-15.
- Kim SY, Matsumi Y, Yasuda T and Mase H. Storm surges along the Tottori coasts following a typhoon. *Ocean Engineering* 2014;**91**:133-145.
- Mastenbroek C, Burgers G and Janssen PAEM. The dynamical coupling of a wave model and a storm surge model through the atmospheric boundary layer. *Journal of Physical Oceanography* 1983;**23**:1856-1866.
- Chen Q, Wang L and Zhao H. An integrated surge and wave modeling system for Northern Gulf of Mexico: simulations for urricanes Katrina and Ivan. *Proceedings of the 31st International Conference on Coastal Engineering* (Hamburg, Germany); 2008. p.1072–1084.
- Choi BH, Eum HM and Woo SB. A synchronously coupled tide-wave-surge model of Yellow Sea. *Coastal Engineering* 2003;**47**:381–398.
- Dietrich JC, Bunya S, Westerink JJ, Ebersole BA, Smith JM, Atkinson JH, Jensen R, Resio DT, Luettich RA, Dawson C, Cardone VJ, Cox

- AT, Powell MD, Westerink HJ and Roberts HJ. A high resolution coupled riverine flow, tide, wind, wind wave and storm surge model for southern Louisiana and Mississippi: part II — synoptic description and analyses of Hurricanes Katrina and Rita. *Monthly Weather Review* 2010;**138**:378-404.
12. Kennedy AB, Westerink JJ, Smith JM, Hope ME, Hartman M, Taflanidis AA, Tanaka S, Westerink H, Cheung KF, Smith T, Hamann M, Minamide M, Ota A and Dawson C. Tropical cyclone inundation potential on the Hawaiian Islands of Oahu and Kauai. *Ocean Modelling* 2012;**52-53**:54-68.
13. Ninh PV. *The storm surge models. UNDP project VIE/87/020*, 1992.
14. Sao NT. Storm surge predictions for Vietnam coast by Delft3D model using results from RAMS model. *Journal of Water Resources and Environmental Engineering* 2008;**23**:39-47.
15. Thuy VTTh. *Storm surge modeling for Vietnam's coast*. Netherlands, Delft Hydraulic, Master's thesis; 2003.
16. Hien NX, Uu DV, Thuc T and Tien PV. Study on wave setup with the storm surge in Hai Phong coastal and estuarine region. *Vietnam National University Journal of Science, Earth Sciences* 2010; **26**:82-89.
17. Thuy NB, Cuong HD, Tien DD, Chien DD and Kim SY. Assessment of changes in sea-level caused by Typhoon No. 3 in 2014 and forecast problems. *Scientific and Technical Hydro-Meteorological Journal* 2014;**647**:16-20. (in Vietnamese)
18. Kim SY, Yasuda T and Mase H. Wave set-up in the storm surge along open coasts during Typhoon Anita. *Coastal Engineering, ASCE* 2010;**57**:631–642.
19. Kim SY, Mori N, Mase H and Yasuda T. The role of sea surface drag in a coupled surge and wave model for Typhoon Haiyan 2013. *Ocean Modelling* 2015; doi:10.1016/j.ocemod.2015.06.004.
20. Mase H, Muto R, Mori N, Kim SY, Yasuda T and Hayashi Y. Storm surge simulation due to Isewan Typhoon using detail meteorological re-analysis data. *Journal of Japan Society of Civil Engineers, Ser. B2 (Coastal Engineering)* 2011;**67**(2):401-405. (In Japanese).
21. Chien DD. *Researching the scientific basis to assess the storm surge in the sea areas from Quang Binh to Quang Nam*. Hanoi. Vietnam: University of Science-Vietnam National University, Ph.D. dissertation ; 2015. (in Vietnamese).
22. Honda T and Mitsuyasu H. Experimental study of wind stress in the sea surface. *Annual Journal of Coastal Engineering* 1980;**27**:90–93. (in Japanese).
23. Donelan M A, Haus BK, Reul N, Plant WJ, Stiassnie M, Graber HC, Brown OB and Saltzman ES. On the limiting aerodynamic roughness of the ocean in very strong winds. *Geophysical Research Letters* 2004;**31**:L18306.
24. Flather R A. A storm surge prediction model for the Northern Bay of Bengal with application to the cyclone disaster in April 1991. *Journal Physical Oceanography* 1994;**24**:172-90.
25. Matsumoto K, Takanezawa T and Ooe M. Ocean Tide Models Developed by Assimilating TOPEX/POSEIDON Altimeter data into hydrodynamical model: a global model and a regional model around Japan. *Journal of Oceanography* 2000;**56**:567-581.
26. Booij N, Ris RC and Holthuijsen L.H. A third-generation wave model for coastal regions, part I, model description and validation. *Journal of Geophysical Research* 1999;**104** (C4):7649–7666.
27. Cavaleri L and Malanotte-Rizzoli P. Wind wave prediction in shallow water: Theory and applications. *Journal of Geophysical Research* 1981;**86**(C2):961-973.
28. Hasselmann S, Hasselmann K, Allender JH and Barnett TP. Computations and parameterizations of the nonlinear energy transfer in a gravity wave spectrum. Part II: Parameterizations of the nonlinear transfer for application in wave models. *Journal of Physical Oceanography* 1985; **15**(11):1378-1391.
29. Battjes JA and Janssen JPFM. Energy loss and set-up due to breaking of random 894 waves. *Proceeding of 16th International Conference Coastal Engineering, ASCE* 1978; p. 569-587.
30. Madsen OS, Poon YK and Graber HC. Spectral wave attenuation by bottom friction: Theory. *Proceeding of 21th International Conference Coastal Engineering, ASCE* 1988; p. 492-504.
31. Schloemer RW. *Analysis and synthesis of hurricane wind patterns over Lake Okechobee*. Washington, U.S. Govt. Print Off, No. 31; 1954.
32. Fujii T and Mitsuta Y. Synthesis of a stochastic typhoon model and simulation of typhoon winds. *Annuals Disaster Prevention Research Institute, Kyoto University, No.29, B-1, 1986; p. 229-239* (in Japanese).